ACADEMIC PRESS

Available online at www.sciencedirect.com

SCIENCE DIRECT®

Journal of Solid State Chemistry 172 (2003) 116–122

JOURNAL OF SOLID STATE CHEMISTRY

http://elsevier.com/locate/jssc

On a new calcium vanadate: synthesis, structure and Li insertion behavior

S. Jouanneau, A. Verbaere,* and D. Guyomard

Laboratoire de Chimie des Solides, Institut des Matèriaux Jean Rouxel, 2, rue de la Houssinière, BP 32229, 44322 Nantes Cedex 03, France

Received 23 July 2002; received in revised form 28 October 2002; accepted 9 November 2002

Abstract

A synthetic form of the mineral hewettite was prepared via a new route in aqueous medium, starting either from the crystalline compound $Li_{1.1}V_3O_8$, or from its amorphous precursor. The anhydrous, crystalline derivative $Ca_{0.5}V_3O_8$ was obtained by heating the synthetic hewettite at 250°C under dynamic vacuum. The diffraction studies show that the 2D structure of $Ca_{0.5}V_3O_8$ involves the same V_3O_8 layers as in the hewettite or in $Li_{1+\alpha}V_3O_8$. The stacking of the layers is similar to that in the metahewettite. A structural model is proposed, where the Ca^{2+} ions occupy octahedral sites in the interlayer space. The electrochemical behavior of $Ca_{0.5}V_3O_8$ vs. lithium insertion is presented. It is original and reveals particularly good performances in terms of stability during cycling at C/5 rate. The homologues obtained with Mg or Ba, instead of Ca, are briefly presented.

Keywords: Vanadium oxide; Vanadate; Calcium; Hewettite; Structure; Lithium insertion; Lithium battery

1. Introduction

$Li_{1+\alpha}V_3O_8$ material has been extensively studied for its lithium insertion properties, as it shows high capacity, acceptable cyclability, and high rate capability [1–4]. This oxide has a layered structure, with the anionic V_3O_8 layers held together by Li^+ ions mainly in octahedral sites in the inter-layer space [5,6]. The lithium ions show ion exchange properties: we previously described the synthesis and the characterization of compounds where Li is partially replaced by divalent Mg, Ca, or Ba cations [7]. The lithium insertion properties of these compounds $Li_{1-2x}M^{II}_xH_yV_3O_8$ (M = Mg, Ca, Ba) being of interest [7], it was deemed worthwhile to prepare and study the fully substituted homologues. As a matter of fact, complete Li–Ca substitutions in $Li_{1+\alpha}V_3O_8$ (α close to 0.1) were obtained during several attempts to prepare $Li_{1.1-2x}Ca_xV_3O_8$ ($0.1 \leqslant x \leqslant 0.3$), thus indicating possible routes of preparation.

With a formula roughly $M_{0.5}V_3O_8$ and with a structure similar to that of $Li_{1+\alpha}V_3O_8$, the expected compounds would be closely related to the hewettite group [8]. Hewettite, $CaV_6O_{16}\cdot 9H_2O$, is a hydrated mineral, with monoclinic symmetry, from which other hydrates with a lower water content have been obtained, in particular the metahewettite $CaV_6O_{16}\cdot 3H_2O$ [9]. A structural study was performed on a sample of hewettite, relatively well crystallized, of composition $CaV_6O_{16}\cdot 7H_2O$ [10]. It reveals that the structure is characterized by the stacking of V_3O_8 layers similar to those in $Li_{1+\alpha}V_3O_8$ and by the presence of Ca and H_2O between the well separated layers. For a review on the crystal data in the hewettite group, see Refs. [9,11].

Several papers have described conditions of precipitation of synthetic members of the hewettite group from aqueous solutions of metavanadates [12–16]. According to the studies of the thermal dehydrations and decompositions, in air, of $MV_6O_{16}\cdot nH_2O$ (M = Mg, Ca, Ba), these hydrates begin to decompose before complete dehydration [17–21]. To our knowledge, the anhydrous forms $M_{0.5}V_3O_8$ have not been isolated nor described in the literature.

Other authors have reported electrochemical and chemical insertion of Li or Mg in solids of composition $MV_6O_{16}\cdot nH_2O$ (M = Mg, Ca) [22–25]. According to the data reported in the Mg case [22], these solids are not hewettite group members.

*Corresponding author. Fax: +33-2-40-37-39-95.
E-mail address: verbaere@cnrs-imn.fr (A. Verbaere).

0022-4596/03/$ - see front matter © 2003 Elsevier Science (USA). All rights reserved.
doi:10.1016/S0022-4596(02)00164-0

This paper is mainly focused on the preparation of the new, anhydrous compound $Ca_{0.5}V_3O_8$, on its structural characterization, and on its lithium insertion behavior. Preliminary results obtained for the Mg and Ba homologues are briefly mentioned.

2. Experimental

The chemical analyses of Li, Mg, Ca, and Ba were performed by inductively coupled plasma atomic absorption spectrometry (ICP-AAS). The oxidation state of V was determined by potentiometric titration using a Ce^{IV} sulfate solution [26]. EDX analyses with a JEOL 5800SV scanning electron microscope (SEM) were used to determine the vanadium and (as a check) the divalent cation contents.

The SEM images of the samples were taken with a JEOL 6400F scanning electron microscope. The TG and DSC analyses were performed using a SETARAM TG-DSC 111 system, at a heating rate of $2\,K\,min^{-1}$, in air.

The line positions and intensities were determined using the program Prolix [27]. The cell parameters were least-squares refined using the program U-Fit [28]. The powder X-ray diffraction (XRD) data were recorded using Cu$K\alpha$ radiation for approximately 15 h, with a Siemens D5000 diffractometer for the hydrated compounds. An INEL system was used for the dehydrated derivatives, which were in a silica capillary tube filled and sealed under argon atmosphere. The selected area electron diffraction (SAED) patterns were obtained using a Philips CM30 microscope.

For the electrochemical study, the positive electrodes were prepared by mild grinding of the active material, followed by mixing with carbon black (Super P from Chemetal) and binder (polyvinylidene difluoride: PVDF) with the massic ratio (85:10:5), and coating the mixture onto an Al disk serving as the current collector, as described in Ref. [29]. Such electrodes were vacuum-dried at 250°C for 1 h before entering a dry Ar glove box. Two-electrode Swagelok™ test cells [30] using the positive electrode, a porous paper soaked with the electrolyte as the separator, and metallic lithium as the negative electrode were assembled in the glove box. A 1 M solution of $LiPF_6$ in ethylene carbonate (EC) and dimethyl carbonate (DMC) (70:30) (Merck) was used as the electrolyte. All voltages given in the text are reported vs. the Li^+/Li negative electrode.

Electrochemical Li insertion and cell cycling were performed at 22°C, and monitored by a Mac-Pile™ system [31] in galvanostatic mode. The voltage range used was 3.7–2 V. A chronoamperometric study in potentiodynamic mode (Potentiostatic Intermittent Titration Technique: PITT) was realized at $20\,mV\,h^{-1}$ during both discharge and charge.

3. Results and discussion

3.1. Synthesis of $Ca_{0.5}V_3O_8 \cdot nH_2O$

An aqueous solution of $Ca(NO_3)_2 \cdot nH_2O$ in large excess (10 times) was prepared with ultra pure water. The precursor first used was $Li_{1.1}V_3O_8$ prepared by annealing at 350°C in air for 10 h a freeze-dried gel obtained according to the procedure proposed by Pistoia et al. [32], and modified by West et al. [33]. This precursor is, hereafter, named SG350. Two hundred milligrams of the precursor was then added to 100 ml of the solution and the suspension was stirred at 50°C for 5 h. The solid product, readily formed, was stable in the aqueous solution; it was separated by filtration, followed by washing with ultra pure water, and dried in air.

In fact, the same product was also obtained by simply using the freeze dried gel as a precursor, i.e. without any thermal treatment. Note the freeze dried gel is amorphous and hydrated, so that the reaction processes between the lithium vanadate and the aqueous solution are necessarily different for the two precursors (gel or SG350).

In the SG350 case, there is no reason to suppose that the reaction is simply a Ca–Li ion exchange. On the contrary, as indicated by the following results, we may suppose that the SG350 phase disappears (for example it could return to a gel form in the aqueous solution) before or during the formation of the final solid. First, the chemical analyses show the final solid product is no longer a bronze. Its V^{IV} and Li contents are negligible. The experimental atomic ratio Ca:V was found in the range 0.46:3–0.48:3, i.e. slightly less than 0.5:3, suggesting the probable presence of a few protons ensuring the electric neutrality in a formula close to $Ca_{0.5}V_3O_8 \cdot nH_2O$. Secondly, Fig. 1 shows the final compound consists of well developed crystals (rods up to 1 μm long Fig. 1a), very different from those of the crystalline precursor SG350 (Fig. 1b). This final aspect is the same whatever the precursor (gel or SG350). These features indicate that crystals of the new phase form and grow during the preparation reaction.

A few tests showed that a hydrothermal route leads to a product which seems identical, when 150 mg of a stoichiometric mixture of V_2O_5 and $Ca(OH)_2$ are held at 200°C in 5 ml of H_2O for 10 days.

3.2. Characterizations

The substituted solid obtained is a hydrate, with a water content which reversibly varies with the relative humidity, and with the temperature, as expected for a layered compound likely similar to the hewettite [34]. TG and DSC analyses were performed for comparison with the previous results, and to determine a thermal treatment to obtain the anhydrous derivative without

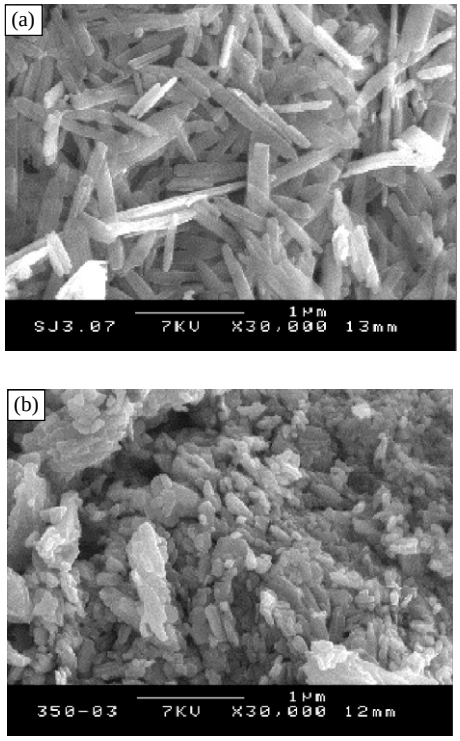

Fig. 1. SEM images of $Ca_{0.5}V_3O_8$ (a), and of the precursor SG350 (b), at the same magnification.

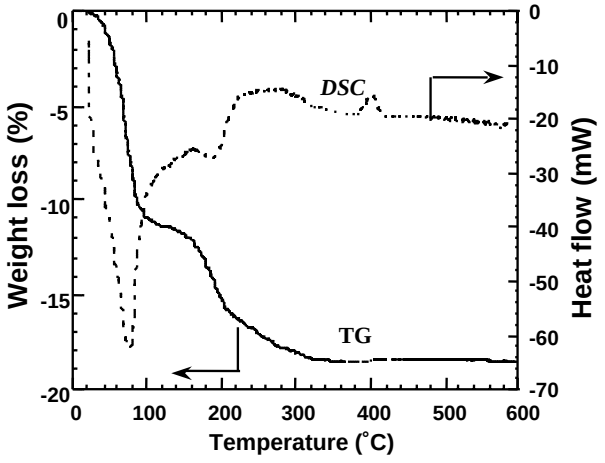

Fig. 2. TG and DSC curves of the Ca hydrated compound (under air, at 2 K min^{-1}).

destruction of the layered structure. The curves of Fig. 2 are quite similar to those reported in Ref. [18] for a synthetic hewettite; they show that the weight loss occurs mainly with two endothermic phenomena around 70°C and 190°C and ends slowly from 220°C to 350°C. The powder XRD pattern of the final product at 590°C shows the formation of a mixture of CaV_2O_6 and α V_2O_5, so that the exothermic peak near 400°C likely corresponds to the irreversible thermal decomposition. Thus, for a complete dehydration while still preserving the layers, a heat treatment at 250°C under dynamic vacuum for 1 h was retained. A TG curve obtained for a sample thus dehydrated showed no residual water loss.

For a formula $Ca_{0.5}V_3O_8 \cdot nH_2O$, the TG curve corresponds to $n = 3.8$, for a sample exposed for several days to the air moisture at room temperature. This water content is intermediate between those previously reported (3.5 [10] and 4.5 [34]) for hewettite. The inflexion point with a pseudo-plateau at 120°C (Fig. 2) indicates the existence of a particular hydrate with $n = 1.5$, which corresponds exactly to the content reported for the metahewettite [35], a less hydrated form of hewettite.

Fig. 3 shows the powder XRD patterns of the hydrated (a), and dehydrated (b) samples, and of $Li_{1.1}V_3O_8$ SG350 (c). The intense line at low 2θ angle indicates the inter-layer distance. The XRD pattern of the hydrated phase is that of a hewettite: it is similar to PDF 84-2134 [10] and almost identical to PDF 35-0564 [36]. The powder XRD pattern of the dehydrated compound $Ca_{0.5}V_3O_8$ presents noticeable similarities with that of the precursor $Li_{1.1}V_3O_8$. However, the cell parameter refinement does not lead to satisfactory results when the starting parameters used are those of $Li_{1+\alpha}V_3O_8$. In particular, some weak diffraction peaks observed cannot be thus explained.

A precise structural study being precluded by the low level of crystallinity, an electron diffraction study was performed, in particular to verify that the periodicity within the layers is close to that in hewettite or $Li_{1+\alpha}V_3O_8$. The crystallites are platelets elongated along the b axis. When the electron beam is nearly perpendicular to the platelet, the diffraction pattern agrees fairly well with the expected layer periodicity with, however, the systematic absences of reflections shown in Fig. 4. The diffraction condition observed is $0k_Il_I : k_I + l_I = 2n$ (assuming the layer periodicity is given by the monoclinic b and c axes as in $Li_{1+\alpha}V_3O_8$). The expected

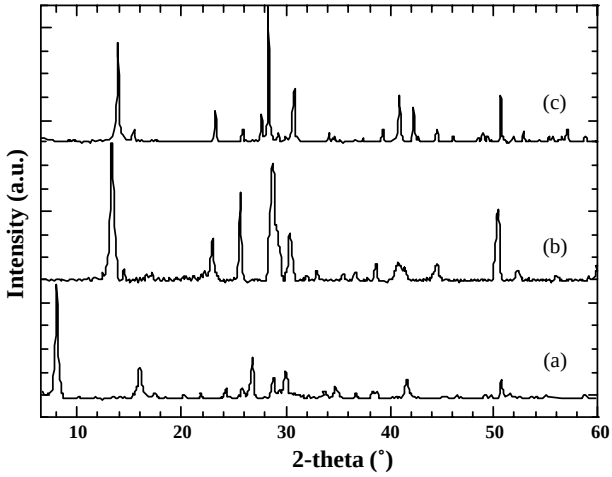

Fig. 3. Powder XRD pattern for: the hydrated calcium phase (a), the dehydrated one (b), and $Li_{1.1}V_3O_8$ SG350 (c).

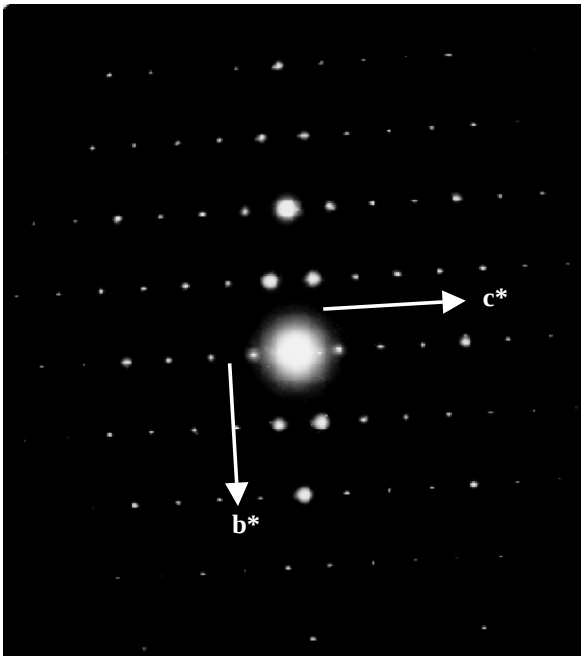

Fig. 4. Electron diffraction (SAED) pattern of $Ca_{0.5}V_3O_8$ ([1 0 0] zone) showing the systematic absence of reflections. The axes are consistent with the unit cell noted I in Fig. 5.

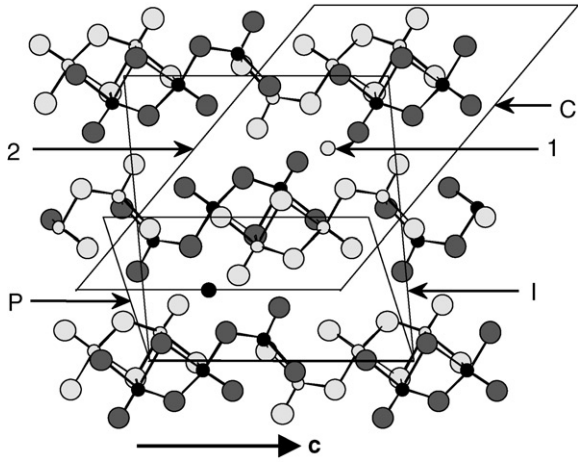

Fig. 5. [0 1 0] view of the hypothetical structure of $Ca_{0.5}V_3O_8$. Small and large circles represent V and O atoms, respectively; light and dark circles indicate $y = 0$ and 1/2, respectively. P indicates the unit cell of $Li_{1+\alpha}V_3O_8$ (space group $P2_1/m$); I and C indicate possible cells for $Ca_{0.5}V_3O_8$ associated with space groups $I2/m$ and $C2/m$, respectively. Site 1 is the hypothetical octahedral site of Ca, and 2 indicates a region of interconnected cavities which form a tunnel parallel to the b axis.

symmetry being monoclinic (or less), the condition is interpreted as coming from the global condition $h_I k_I l_I$: $h_I + k_I + l_I = 2n$ (where the subscript I indicates a body centered lattice), which implies a particular stacking of the V_3O_8 layers: as compared to the hewettite and $Li_{1+\alpha}V_3O_8$ (space group $P2_1/m$), every second V_3O_8 layer is shifted by $b/2$. The relevant conventional space group is $C2/m$, and the unit-cell shown in Fig. 5 is consistent with this symmetry. This figure illustrates the hypothetical structure we propose for $Ca_{0.5}V_3O_8$. It was obtained in the following manner:

(1) the V_3O_8 layers are those in $Li_{1+\alpha}V_3O_8$ (similar to those in hewettite), i.e. they are built from chains of VO_6 or VO_5 polyhedra (see Fig. 5) sharing edges and vertices, and running parallel to the b axis [5,6];
(2) they are stacked according to the $C2/m$ symmetry;
(3) owing to the XRD pattern the interlayer distance is 6.65 Å;
(4) the β angle retained is the one consistent with acceptable O–O distances between oxygen atoms of adjacent layers. This angle leads to an octahedral site fairly well adapted to Ca, which was supposed to occupy this site.

With this hypothetical structure, the cell-parameter refinement is satisfactory and all the lines of the XRD pattern are explained (Table 1). Fig. 6 shows the powder XRD patterns: (a) experimental and (b) calculated using the program PowderCell [37], with the hypothetical structure and the cell parameters: $a = 17.66(1)$ Å, $b = 3.621(1)$ Å, $c = 12.346(6)$ Å, $\beta = 131.15(4)^\circ$ (consistent with space group $C2/m$). Note the layer parameters b and c are slightly larger as compared to $Li_{1.1}V_3O_8$ ($b = 3.5932(3)$, $c = 11.993(1)$), and the structure contains tunnels, parallel to the b axis (see region 2 in Fig. 5), and well adapted to a high mobility of Li.

3.3. *Electrochemical Li insertion properties of $Ca_{0.5}V_3O_8$*

The electrochemical behavior vs. lithium insertion has been studied for $Ca_{0.5}V_3O_8$. The variation of the voltage vs. insertion capacity obtained for this compound during the first two cycles at $C/50$ rate is presented in Fig. 7(a). The total inserted capacity expressed as a number x of Li per formula unit is 2.8 Li during the first discharge (the complete reduction of V^V to V^{IV} corresponds to $x = 3$). This capacity of 2.8 Li is not fully recovered (only 1.9 Li) during the subsequent charge. The subsequent cycles are similar to the second one, shown in Fig. 7(a) with dotted lines. The incremental capacity, deduced by derivation of Fig. 7(a), is presented in Fig. 7(b) for the two first cycles. The first discharge is marked by two phenomena: the first one by a broad peak which occurs about 3 V and the second one by a narrow peak at 2.50 V. During the first charge, an equivalent of this narrow peak is observed, slightly shifted from 2.50 to 2.58 V, but there is no equivalent of the broad 3 V discharge peak; only some residual current is measured between 3.0 and 3.7 V. During the second cycle the 3 V broad peak observed at first discharge is replaced by a shoulder at 2.8–2.9 V, and the main phenomenon is detected at ~2.53 V. Thus the irreversible loss of capacity at the first discharge mainly

Table 1
Powder XRD data for $Ca_{0.5}V_3O_8$; $a = 17.66$ Å, $b = 3.621$ Å, $c = 12.346$ Å, $\beta = 131.15°$; space group $C2/m$

h	k	l	d_{obs} (Å)	d_{calc} (Å)	I/I_0	h	k	l	d_{obs} (Å)	d_{calc} (Å)	I/I_0
0	0	1	9.249	9.296	15	8	0	−3	2.176	2.179	14
2	0	0	6.632	6.647	100	−5	1	5	2.035	2.038	14
2	0	−2	6.137	6.164	5	0	0	5	1.857	1.859	6
4	0	−3	3.870	3.867	25	0	2	0	1.810	1.810	49
−1	1	1	3.471	3.474	40	2	2	0	1.748	1.747	13
1	1	1	3.105	3.099	98	4	2	−3	1.639	1.640	3
−3	1	1	3.059	3.060	25	4	2	−4	1.561	1.561	8
−3	1	2	3.026	3.021	38	−6	2	3	1.541	1.541	16
6	0	−3	2.936	2.934	51	6	0	−8	1.521	1.519	13
3	1	−3	2.713	2.717	6	7	1	1	1.509	1.508	2
5	1	−2	2.525	2.520	6	6	2	−1	1.480	1.480	5
4	0	−5	2.448	2.448	4	−4	2	5	1.456	1.456	11
3	1	−4	2.326	2.328	12	2	2	−5	1.399	1.400	21
2	0	−5	2.209	2.206	34						

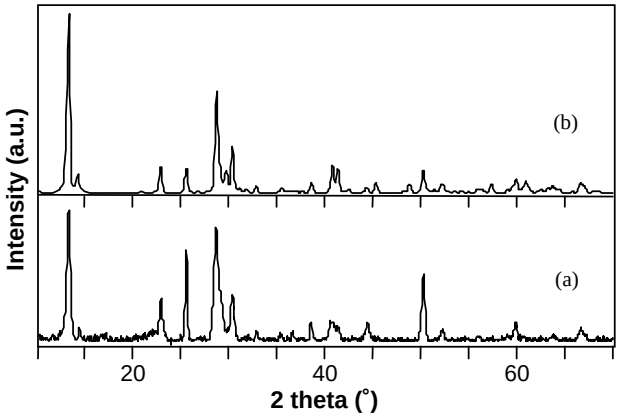

Fig. 6. Powder XRD patterns of $Ca_{0.5}V_3O_8$: experimental (a); calculated with the proposed structure (b).

concerns the phenomenon around 3 V. During the next cycles the 2.8–3.0 V process has totally disappeared.

The PITT study (see Fig. 8) confirms the phenomena of the first cycle, and gives more detailed information. At voltages between 3.2 and 2.8 V, the $I_f - t$ peak (I_f is the current at the end of each voltage step), and thus the $I_f - V$ peak, has an asymmetrical shape (see Fig. 8a). Moreover, the shape of the absolute current decay with time is different in the ascending part and in the descending part of the peak. It is the signature of a first order transformation [38,39]. The shape of the current decay with time in the ascending part of the peak gives information on the kinetics of the 3 V process, as well. The quasi-linear current variation indicates that the Li insertion process is kinetically limited by Li diffusion within the new phase that forms at the surface of the grains [38,39]. The same observations apply to the reversible 2.5 V discharge (see Fig. 8a) and charge process (Fig. 8b), thus indicating that its Li insertion mechanism is also two phased with a kinetic limitation by Li diffusion in the new phase.

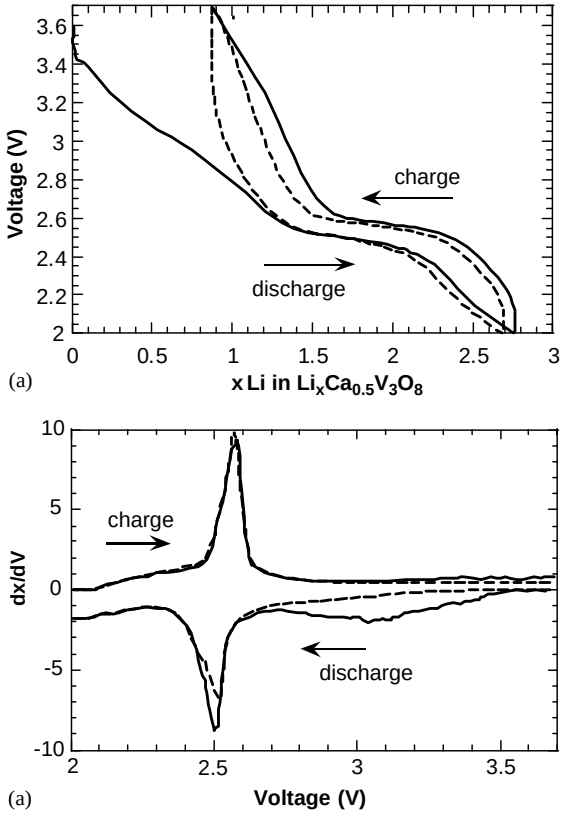

Fig. 7. Voltage versus Li composition (a) and incremental capacity versus voltage (b) curves obtained for $Ca_{0.5}V_3O_8$ during the first two discharge-charge cycles in galvanostatic mode at $C/50$ rate.

The cycling behavior of $Ca_{0.5}V_3O_8$ is presented in Fig. 9. The initial rate was $C/50$ for the first two cycles, followed by a few cycles at $C/20$, and finally cycles at $C/5$. This increase of the cycling rate leads to a small capacity drop, indicating that the measured capacity has a slight kinetic limitation. Apart the initial capacity loss, the capacity of 125 mA h g^{-1} remains constant upon cycling at $C/5$. The major capacity drop comes from the

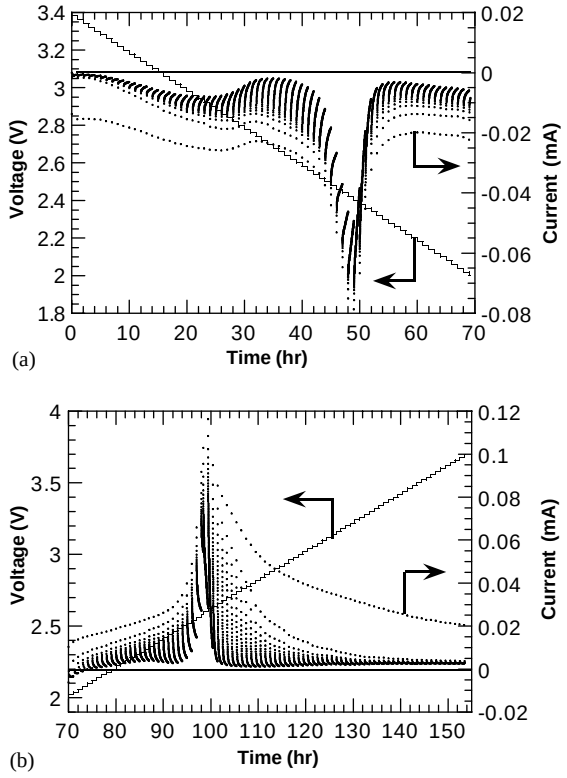

Fig. 8. PITT curves with chronoamperometric evolutions obtained for $Ca_{0.5}V_3O_8$ during the first discharge (a) and the first charge (b).

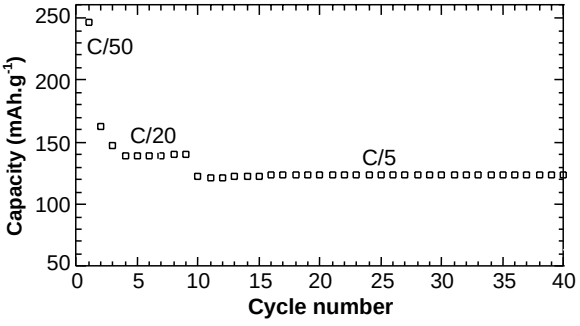

Fig. 9. Variation of the capacity, expressed in $mA\,h\,g^{-1}$, recorded during galvanostatic cycling at various successive rates (the two first at $C/50$, followed by a few at $C/20$ and finally at $C/5$ in discharge ($C/10$ in charge)).

irreversible loss of capacity at the first cycle, due to the irreversibility of the 3 V two phase transformation leading to 0.9 Li per formula unit trapped in the structure.

3.4. Remarks on the Mg and Ba homologues of $Ca_{0.5}V_3O_8$

When the preparations were performed using $Mg(NO_3)_2$ or $Ba(NO_3)_2$ instead of $Ca(NO_3)_2$ for the reaction with $Li_{1.1}V_3O_8$, the solids obtained also showed the behavior of layered hydrates, as in the Ca case. These Mg or Ba compounds are of lower crystallinity.

Table 2
Unit-cell parameters (monoclinic symmetry) refined for the dehydrated phases. b and c give the layer periodicity

M	a (Å)	b (Å)	c (Å)	β (°)	Δ (°)
Mg	17.66 (1)	3.601(2)	12.107(9)	127.27(7)	0.026
Ca	17.66(1)	3.621(1)	12.346(6)	131.15(4)	0.018
Ba	18.47(6)	3.611(3)	12.33(2)	129.3(2)	0.037

Δ is the mean error in 2θ.

The powder XRD pattern of the Mg compound is quite similar to that given in Ref. [12] for $MgV_6O_{16}\cdot 9H_2O$ (PDF 46-0281). The powder XRD patterns of the hydrated or dehydrated samples are rather well explained assuming their structure is similar to that of the title Ca compound, since the cell parameter refinements for samples dehydrated at 250°C for 1 h under dynamic vacuum lead to the results in Table 2.

The EDX analyses of V and M (M = Mg or Ba) in several samples, however, revealed (i) significant variations of the $M:V$ ratio, and (ii) values of $M:V$ in the range 0.54:3–0.60:3, i.e. values significantly higher than that expected, so that more work is still needed concerning the formulas and the structures of these phases. Note an atomic ratio $M:V$ of 0.6:3 was already reported for a Ba member of the hewettite group [11]. The Mg and Ba compounds were arbitrarily dehydrated at 250°C for 1 h, as for $Ca_{0.5}V_3O_8$. Preliminary tests showed the electrochemical behaviors of these Mg and Ba samples are similar to that of $Ca_{0.5}V_3O_8$. The smaller the cation, the larger the reversible capacity at the first cycle. No cycling capability has been obtained for the Mg compound, probably due to the presence of residual water despite the thermal treatment. For the Ba compound, the capacity is constant on cycling at $C/5$ rate but smaller than that obtained for $Ca_{0.5}V_3O_8$ (0.9 Li for Ba instead of 1.4 for Ca).

4. Conclusion

Via a new route, a compound of composition close to $Ca_{0.5}V_3O_8\cdot nH_2O$ was prepared in aqueous medium. It appears as a synthetic hewettite. Its structure together with that of the new, anhydrous derivative $Ca_{0.5}V_3O_8$ are closely related to that of $Li_{1+\alpha}V_3O_8$. The structural model described for $Ca_{0.5}V_3O_8$ is original and agrees with the observations from the diffraction studies. Mg and Ba compounds have the parent structure. Some further complementary experiments are necessary to determine their exact composition.

The three dehydrated compounds, with Mg, Ca, or Ba, have been studied vs. lithium insertion. They exhibit good lithium insertion properties, prior to any optimization. The complete study performed for $Ca_{0.5}V_3O_8$ shows an original behavior, i.e. different from that of

$Li_{1+\alpha}V_3O_8$. The calcium compound $Ca_{0.5}V_3O_8$ shows one main reversible two-phase Li insertion phenomenon. It has the best behavior, particularly in terms of cycling with a stable capacity of $125\,mA\,h\,g^{-1}$ at $C/5$ rate.

Acknowledgments

The authors thank EDF for financial support. S. Jouanneau is also grateful for the research fellowship provided by the DGA.

References

[1] D. Guyomard, In: T. Osaka, M. Datta (Eds.), New Trends in Electrochemical Technology: Energy Storage Systems in Electronics, Gordon and Breach, Philadelphia, 2000, pp. 253–350 (Chapter 9).
[2] K. Nassau, D.W. Murphy, J. Non-Cryst. Solids 44 (1981) 297.
[3] G. Pistoia, S. Panero, M. Tocci, R.V. Moshtev, V. Manev, Solid State Ion. 13 (1984) 311.
[4] G. Pistoia, M. Pasquali, M. Tocci, V. Manev, R.V. Moshtev, J. Power Sources 15 (1985) 13.
[5] A.D. Wadsley, Acta Crystallogr. 10 (1957) 261–267.
[6] L.A. de Picciotto, K.T. Adendorff, D.C. Liles, M.M. Thackeray, Solid State Ion. 62 (1993) 297–307.
[7] S. Jouanneau, A. Le Gal La Salle, A. Verbaere, D. Guyomard, M. Deschamps, S. Lascaud, New Mater. Electrochem. Systems 5 (2002) 191–196.
[8] H.T. Evans, Miner. Magn. 46 (1982) 503.
[9] H.T. Evans, J.M. Hughes, Am. Miner. 75 (1990) 508–521.
[10] H.T. Evans, Can. Miner. 27 (2) (1989) 181–188.
[11] Y. Oka, T. Yao, S. Sato, N. Yamamoto, J. Solid State Chem. 140 (1998) 219–225.
[12] L. Zurkova, C. Goczeova, E. Drobna, S. Korenkova, Chem. Pap. 43 (1) (1989) 9–16.
[13] L. Ulicka, V. Sucha, Chem. Zvesti. 38 (1) (1984) 85–89.
[14] A.K. Il'yasova, R.A. Geskina, G.K. Tarabrin, N.D. Omarova, V.A. Biryukova, A.V. Ekshtelis, Zh.K. Zhubatov, Zh. Neorg. Khim. 28 (7) (1983) 1666–1669.
[15] T. Tkac, L. Zurkova, Chem. Zvesti. 33 (6) (1979) 749–757.
[16] I.G. Chufarova, A.A. Ivakin, N.I. Petunina, L.A. Perelyaeva, O.V. Koryakova, Zh. Neorg. Khim. 24 (4) (1979) 953–957.
[17] C. Goczeova, J. Therm. Anal. 36 (1) (1990) 137–144.
[18] L. Zurkova, Acta Fac. Rerum Nat. Univ. Comenianae, Chim. (1987) 34 (1986) 75–86.
[19] L. Zurkova, V. Sucha, Thermochim. Acta 98 (1986) 255–262.
[20] L. Zurkova, V. Sucha, Proc. Conf. Coord. Chem. 10 (1985) 523–528.
[21] O.V. Koryakova, L.A. Perelyaeva, E.V. Zabolotskaya, N.I. Medvedeva, A.A. Ivakin, Zh. Neorg. Khim. 27 (10) (1982) 2521–2525.
[22] P. Novak, V. Shklover, R. Nesper, Z. Phys. Chem. 185 (1) (1994) 51–68.
[23] P. Novak, W. Scheifele, O. Haas, Molten Salt Forum 1 (2) (1993/1994) 389–396.
[24] P. Novak, W. Scheifele, O. Haas, J. Power Sources 54 (1995) 479–482.
[25] P. Novak, W. Scheifele, F. Joho, O. Haas, J. Electrochem. Soc. 142 (8) (1995) 2544–2550.
[26] F. Théobald, Ph.D. Thesis, Besançon, 1975.
[27] M. Evain, J.M. Barbet, P. Deniard, R. Brec, Powder Diffraction Meeting, Toulouse, France, 1990.
[28] M. Evain, U-FIT Manual, Institut des Matériaux de Nantes Internal Report, Nantes, France, 1992.
[29] F. Leroux, D. Guyomard, Y. Piffard, Solid State Ion. 80 (1995) 30.
[30] J.M. Tarascon, J. Electrochem. Soc. 132 (1985) 2089.
[31] C. Mouget, Y. Chabre, MacPile, licensed from CNRS and UJF Grenoble to BioLogic Co, 1 av. de l'Europe, F-38640 Claix.
[32] G. Pistoia, M. Pasquali, G. Wang, L. Li, J. Electrochem. Soc. 137 (8) (1990) 2365.
[33] K. West, B. Zachau-Christiansen, J. Electrochem. Soc. 143 (3) (1996) 820.
[34] M.M. Qurashi, Can. Miner. 6 (1961) 647–662.
[35] P. Bayliss, S.J. Warnes, Miner. Magn. 43 (1979) 550.
[36] P. Bayliss, Miner. Magn. 46 (1982) 503.
[37] W. Kraus, G. Nolze, Federal Institute for Materials Research, Berlin, Germany, 1999.
[38] D. Djurado, M. Barral, Y. Chabre, J.E. Fisher, In: P. Bernier (Ed.), Chemical Physics of Intercalation II, Plenum Press, New York, 1993, p. 255.
[39] Y. Chabre, Conference at Workshop on Electrochemistry and Material, organized by CNRS, Amiens, May 2001.